2000 IEEE/EIA International Frequency Control Symposium and Exhibition

THERMAL TRANSIENT STUDIES OF ANHARMONIC SENSORS OF AGING OF PRECISION AT-CUT CRYSTAL RESONATOR

Yuriy S Shmaliy, Guanajuato Univ., Salamanca, Gto, Mexico
Anatoliy V Marienko, Oleksandr Ph Kurotchka, "Sichron" Center, Kharkiv, Ukraine
Miguel Torres-Cisneros, Oscar Ibarra-Manzano, Guanajuato Univ., Salamanca, Gto, Mexico

Abstract

The report addresses the thermal transient of the sensor of aging (anharmonic mode h_{513} of AT-cut crystal resonator) of the crystal standard based on the modulational method. The thermal dynamic properties of the aging sensor influence the effect of the aging compensation for the standard. We present the thermal model of a crystal resonator and consider in detail the model of the thermally induced frequency transient in a resonator within the ovenized oscillator. The model has been examined for the aging sensor excited by modulation within the Colpitts oscillator. Based on the model, we digitally simulate the anticipated behavior of the thermally induced frequency of the aging sensor and compare it with that obtained by measurement. Finally, we show how to compensate the temperature dependence of the aging code of the standard.

Introduction

The recently proposed modulational method [1] has proven to be an effective way to achieve computerized aging rate compensation as realized in the Ch1-88 type crystal standard [2]. In this standard, the output frequency behaves in time as rather a stationary random process instead of a non-stationary one as in traditional crystal oscillators. Although the aging behavior is improved, random frequency variations may be increased because of the aging sensor temperature sensitivity (~1 Hz/°K). Studying this effect, one may conclude that it may be strongly reduced by digital filtering of the temperature-induced variations of the digital compensating voltage formed by the aging sensor. It is obvious, however, that a thermal impulse response of the aging sensor is necessary to make digital filtering and that inaccuracies in the response result in a frequency behavior with a filtering.

Attempts to create dynamic thermal models for the crystal resonator had been undertaken more than once [3]—[6]. Nevertheless, only Ivlev's dynamic thermal frequency coefficient for a frequency domain [3] and Ballato's $\tilde{a}$ coefficient [4] for a time domain of temperature changes have gained currency. Holland in [5], [6] and others [7]—[10] have carried out theoretical investigations of resonator frequency processes resulting from the influence of ambient temperature dynamics. Of special significance is the work of Valentin *et al.* [11], who presented results of experimental studies of thermal flows and their contributions to the processes of heat transport for vacuum-enclosed resonators. The results of this and other papers had been used further for the evaluation of thermal dynamic frequency changes in a self-contained crystal plate [12]—[14]. At present, these theoretical and practical materials allow us to work out the model of a thermally induced frequency transient of a vacuum-enclosed resonator as it reacts to a step change in ambient temperature.

In this report we deal with thermal dynamic properties of the anharmonic sensor of aging being based on a physical analysis of thermal processes in both resonator and oscillator within an oven system. First, we present the improved thermal model of a crystal resonator within an oscillator, consider in detail the model of a thermally induced frequency transient, and show its correspondence with the Ballato's coefficient. Then, we verify the model by experimentally. Finally, we present the simulation results of the digital filtering of temperature for the aging sensor frequency and show how to compensate a temperature dependence of an aging code of the standard.

Thermal Model of a Crystal Resonator

Let us consider the basic design of a precision vacuum-enclosed quartz crystal unit employing thickness-shear vibrations and operating under the temperature influence within an OCXO. Let us also select a crystal plate, crystal holders (*A*), and an enclosure (*E*) as the main resonator parts (Fig.1). Here, both principal and aging sensor modes exist within a crystal plate volume.

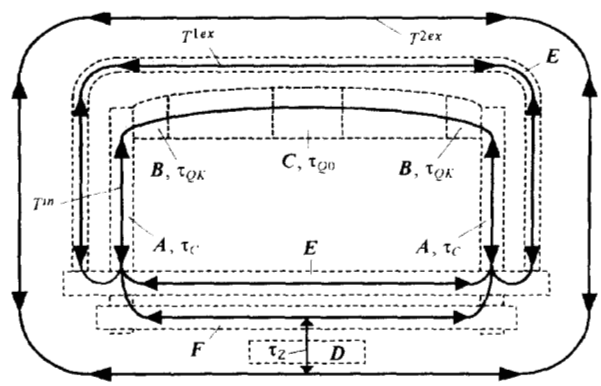

Figure 1. Thermal model of a crystal resonator

0-7803-5838-4/00/$10.00 © 2000 IEEE

Taking the early measurement results obtained by Valentin *et. al.* [9], let us separate the general thermal flows in a vacuum-enclosed resonator as follows: T^{in} is the internal flow that forms a closed path through the parallel parts of the oscillator electronic plate (***F***) and resonator enclosure (***E***), crystal holders (***A***), and piezoelectric plate; T^{1ex} is the first external flow that closes itself through the resonator enclosure, T^{2ex} is the second external flow that is formed by the oscillator body. In addition, we note, that there may be more than one external flow in the OCXO compared with the resonator. Because the heat transfer and exchange by radiation is a rather small effect in vacuum-enclosed crystal units [13], the model of the main resonator thermal circuits may be presented as shown by the following parts (Fig. 1): ***A*** is a part of the crystal holder, ***B*** and ***C*** are, respectively, the edges and center of a crystal plate. In the general case, it is very difficult to simulate the interface between the oscillator and resonator. Let us mark this as ***D*** and give it the character of a delay line with τ_Z response time for thermal exchange between T^{2ex} and T^{in}. With this definition, $\tau_Z = 0$ if the resonator has only one external circuit (i.e., direct contact of the enclosure to the ambient).

Partial Functions of a Thermal Transient

Considering a crystal holder as a thin shaft with coordinate axes beginning from the point of contacts with a piezoelectric plate, let us write the thermal conductivity equation in the form of $\frac{\partial u}{\partial t} = \frac{k_c}{c_c \rho_c} \frac{\partial^2 u}{\partial x^2}$, where u is an environment temperature, $0 \le x \le l$ is a current coordinate, l is a crystal holder length, k_c and c_c, ρ_c are, respectively, the heat conductivity coefficient, specific heat, and density of the holder material, t is a current time. For vacuum enclose one may consider the sides and crystal holder part at the point $x = 0$ as heat insulated and the parts at the point $x = l$ as supported with the surrounding temperature $\widetilde{u}_1$. Such limitations determine the boundary conditions in the forms of $\left.\frac{\partial u}{\partial x}\right|_{x=0} = 0$ and $u|_{x=l} = \widetilde{u}_1$. For the uniform initial conditions $u_{t=0} = u_0$, the solution at the point $x = 0$ is given as

$$u(t) = \widetilde{u}_1 + \frac{4\Delta u}{\pi} \sum_{n=0}^{\infty} \frac{(-1)^n}{2n+1} e^{-\frac{(2n+1)^2 t}{\tau_c}}, \qquad (1)$$

where $\Delta u = u_0 - \widetilde{u}_1$ and $\tau_c = 4l^2 c_c \rho_c / \pi^2 k_c$. Calculations show that neglecting all terms in (1), excluding the first ($n = 0$), results in time-averaged error no more than a few percents. Thus, for the thermal transient model we may use an approximate solution in a form of

$$\Delta u_1 \cong \Delta\widetilde{u}\left(1 - e^{-\frac{t}{\tau_c}}\right), \qquad (2)$$

where $\Delta u_1(t) = u_1(t) - \widetilde{u}_1$, $u_1(t)$ is (1) for $n = 0$, and $\Delta\widetilde{u}$ is the temperature increment.

The thermal transient in a crystal plate is described by the conductive equation [9], [14]

$$c\rho \frac{du}{dt} - \mathrm{div}(\kappa \mathrm{grad} u) = F(x,y,z,t), \qquad (3)$$

where c, ρ, and κ are, respectively, the specific heat, density, and heat conductivity of quartz, $F(x,y,z,t)$ is a function of the internal sources of heat.

In cylindrical coordinates r, φ, *and* z relative to a disk-shaped piezoelectric plate (Fig. 1), the solution of the equation (3) has the form [14]

$$u = u_0 + \Delta u + \sum_{k=0}^{\infty}\sum_{m=0}^{\infty}\sum_{l=0}^{\infty}\left(a_{kml} - b_{kml} e^{-\frac{t}{\tau_{kml}}}\right)\chi_{kml}(r,\varphi,z), \qquad (4)$$

where u_0 and Δu are the initial environmental temperature and its increment and k, m, and l are integer numbers corresponding to $\chi_{kml}(r,\varphi,z)$ basic functions in the directions of z, φ, and r, respectively, employed in the Fourier method solution of (3). Here also a_{kml} and b_{kml} are Fourier coefficients, and τ_{kml} are the response times of the system of functions. Particular solutions of (3) for different types of piezoelectric plates are given in [5], [11]—[14].

Eq. (4) describes the temperature behavior both at the center ($r = 0$) and at the edges ($r = R$) of a crystal plate. For a solution error of a few percents, one may restrict the solution (4), as in the case of (2), with an approximation of the form

$$\Delta u_{QK,Q0} \cong \Delta u\left(1 - e^{-\frac{t}{\tau_{QK,Q0}}}\right), \qquad (5)$$

where $\Delta u_{QK,Q0} = u_{QK,Q0} - u_0$ and τ_{QK} and τ_{Q0} are, respectively, response times for the edges and the center of the crystal plate.

The Model of a Thermally Induced Frequency Transient

Based on the previously mentioned reasoning, let us create a model for the thermally induced resonator transient. For the conversion of a temperature difference between the center and edges of a piezoelectric plate $\Delta u_Q = u_{Q0} - u_{QK}$ to the frequency change $\Delta f(\Delta u_Q)$ that is caused by the force-frequency effect in quartz crystals [16], we will use the following function [13]

$$\delta f(\Delta u_Q) = 2\beta_q H D a_f K_f(\varphi) \Delta u_Q, \qquad (6)$$

where $\beta_f = 3.85\times10^6\ NK^{-1}m^{-2}$, $a_f = f_0\eta / Dn$, H and D are, respectively, the thickness and diameter of the crystal plate; f_0 is the vibration frequency of the resonator; $\eta \approx 1$ is a correction coefficient, n is the resonator mechanical harmonic number, $K_f(\varphi)$ is the value of Rataiski coefficient averaged over φ [16].

Operator model

Let us define an operator circuit model of the resonator in the form of a converter of ambient temperature variations ΔT into frequency changes δf (Fig.2), considering the dynamic thermal model (Fig.1).

The delay operator for the part ***D*** is described as

$$K_Z(p) = k_z e^{p\tau_z} , \quad (7)$$

where p is the Laplace operator, k_Z is the attenuation coefficient for environment temperature influence describing the effectiveness of the heat isolation ($k_z < 1$) and oven ($k_z << 1$) systems of an OCXO.

Circuit gains that correspond to the crystal holders $K_C(p)$ (***A***), crystal plate edges $K_{QK}(p)$ (***B***), and the center of the crystal plate $K_{Q0}(p)$ (***C***) may be written according to (2) and (5) in the form of

$$K_{C,QK,Q0}(p) = \frac{k_{C,QK,Q0}}{1 + p\tau_{C,QK,Q0}} , \quad (8)$$

where, for vacuum-enclosed resonators, one may take $k_{C,QK,Q0} \cong 1$. Gain $K_Q(p)$ corresponds to the static piezoelectric plate temperature T_l that causes a change of frequency described by the nonlinear static frequency-temperature characteristic of a resonator within an oven

$$\delta f_l(t) = \eta_1[T_l(t)] = c_1 T_{ov}(t) + c_2 T_{ov}^2(t) + c_3 T_{ov}^3(t) , \quad (9)$$

where $T_{ov} = T_l - T_0$; c_1, c_2, and c_3 are the polynomial approximation factors; and T_0 is the reference temperature (T_0 = 20°C at NTP).

A temperature difference $\Delta T_D = \Delta T_{Q0} - \Delta T_{QK}$ is transformed into a dynamic frequency change δf_D via a coefficient

$$S_R = \frac{\delta f_D}{\Delta T_D} \quad (10)$$

that is obtained by (6) as $S_R = 2\beta_q HDa_f \overline{K_f(\varphi)}$.

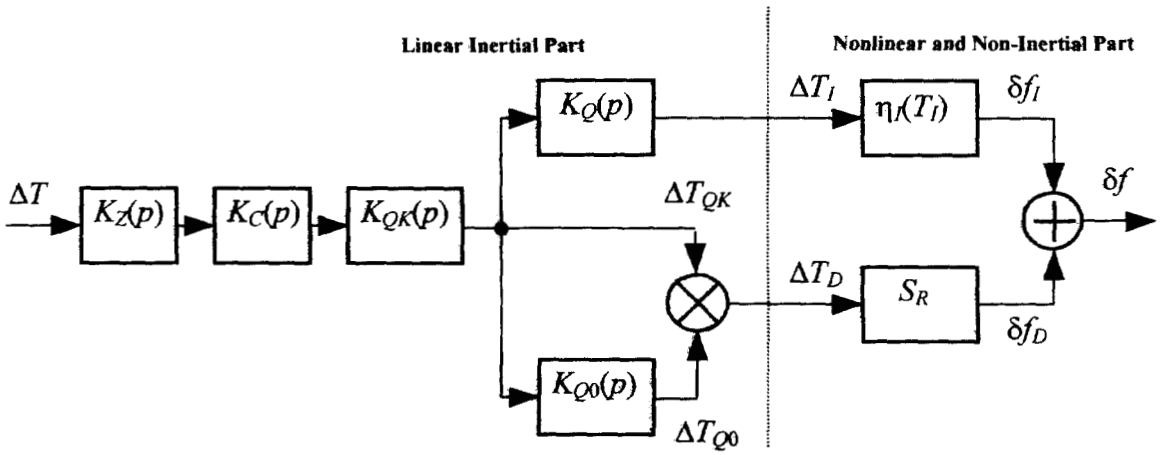

Figure 2. Thermal dynamic operator model of a crystal resonator

"Dynamic" thermal transient

Let us consider a "dynamic" thermal transient ΔT_D, in a resonator. Here and below, we use time solutions of operator equations (7) and (8).

After a temperature step ΔT, the crystal holders and crystal plate edges start to warm-up dependent on delay time τ_Z (7) and response times τ_C and τ_{QK} (8) by the law obtained by the model [19] (Fig. 2)

$$\Delta T_{QK}(t) = \Delta T k_Z k_C k_{QK} \left(1 - a_1 e^{-\frac{t-\tau_Z}{\tau_C}} + a_2 e^{-\frac{t-\tau_Z}{\tau_{QK}}} \right), \quad (11)$$

where $a_1 = \tau_C / (\tau_C - \tau_{QK})$, and $a_2 = \tau_{QK} / (\tau_C - \tau_{QK})$.

The function for a temperature change at the center of the crystal plate is obtained by the model as

$$\Delta T_{Q0}(t) = -\Delta T k_Q \left(1 - b_1 e^{-\frac{t-\tau_Z}{\tau_C}} - b_2 e^{-\frac{t-\tau_Z}{\tau_{QK}}} - b_3 e^{-\frac{t-\tau_Z}{\tau_{Q0}}} \right), \quad (12)$$

where $b_1 = \tau^2_C(\tau_{QK} - \tau_{Q0}) / Y$, $b_2 = \tau^2_{QK}(\tau_{Q0} - \tau_C)$, $b_3 = \tau^2_{Q0}(\tau_C - \tau_{QK}) / Y$, $k_Q = k_Z k_C k_{QK} k_{Q0}$, and $Y = \tau^2_C(\tau_{QK} - \tau_{Q0}) + \tau^2_{QK}(\tau_{Q0} - \tau_{QK})$.

The law describing the temperature difference between the center and ages of the plate may be derived using (11) and (12) with $k_{Q0} \cong 1$, which holds true for vacuum-enclosed resonators, and may be written as

$$\Delta T_D(t) = -\Delta T k_Z k_C k_{QK} \left(v_1 e^{-\frac{t-\tau_D}{\tau_C}} + v_2 e^{-\frac{t-\tau_D}{\tau_{QK}}} + v_3 e^{-\frac{t-\tau_D}{\tau_{Q0}}} \right), \quad (13)$$

where $v_1 = -\frac{\tau_C}{\tau_C - \tau_{QK}} + \frac{\tau^2_C(\tau_{QK} - \tau_{Q0})}{Y}$,

$v_2 = \frac{\tau_{QK}}{\tau_C - \tau_{QK}} + \frac{\tau^2_{QK}(\tau_{Q0} - \tau_C)}{Y}$, and $v_3 = \frac{\tau^2_{Q0}(\tau_C - \tau_{QK})}{Y}$.

Based on (13) and (10), a "dynamic" frequency transient is written as

$$\delta f_D(t) = S_R \Delta T_D(t) , \quad (14)$$

"Static" thermal transient

First, let us note that the amplitude distribution of resonator vibrations is given by the law [17]

$$v_{npq} = e^{-x^2\frac{\alpha_n}{2}}\mathbf{H}_p(x\sqrt{\alpha_n})e^{-z^2\frac{\beta_n}{2}}\mathbf{H}_q(z\sqrt{\beta_n}), \qquad (15)$$

where n is the mechanical harmonic number, x and z are the coordinate axes in the plane of the piezoelectric plate, p and q are indices of the anharmonic vibrations, α_n and β_n are determined in [17], and $\mathbf{H}_p$ and $\mathbf{H}_q$ are Hermite polynomials.

It follows from (15) that vibration modes exist within different areas of a crystal plate and nonuniformly distributed temperature should influence differently the principal and anharmonic sensor modes [18]. Nevertheless, we consider here only the case matched with Ballato's model [4], in which case, a temperature averaged over the crystal plate volume causes the static temperature difference ΔT_1. As this temperature must be static by definition (9) but is changed in time by a transient, we call it the "static" temperature.

Let us define the "static" thermal transient. According to Fig.2, the response $\Delta T_1(t)$ to an input temperature step ΔT change is determined by the operator gain $K_1(p) = K_Z(p)K_C(p)K_{QK}(p)K_Q(p)$. For the averaged temperature of resonator, the transient function has a form

$$g_1(t) = \frac{u(r,\varphi,z,t) - u(r,\varphi,z,0)}{u(r,\varphi,z,\infty) - u(r,\varphi,z,0)}, \qquad (16)$$

where $u(r,\varphi,z,t) = \frac{1}{2\pi RH}\int_0^R\int_0^{2\pi}\int_0^H u(r,\varphi,z,t)drd\varphi dz$ is average temperature obtained by (4) and $\tau_Z \le t$. This model is used for all vibration modes, which have maximums (15) in different zones of a resonator volume. To determine $g_1(t)$, we average a plate "dynamic" temperature (13) as follows: $\int_{\tau_Z}^{t}\Delta T_D(t)dt = -\Delta T_R\Phi g_1(t)$, where $\Phi = v_1\tau_C + v_2\tau_{QK} + v_3\tau_{Q0}$, $T_R = \Delta T k_Z k_C k_{QK}$, and

$$g_1(t) = 1 - \frac{1}{\Phi}\left(v_1\tau_C e^{-\frac{t-\tau_Z}{\tau_C}} + v_2\tau_{QK}e^{-\frac{t-\tau_Z}{\tau_{QK}}} + v_3\tau_{Q0}e^{-\frac{t-\tau_Z}{\tau_{Q0}}}\right), \qquad (17)$$

Based on (17), we find out a "static" thermal transient $\Delta T_1(t) = \Delta T k_1 g_1(t)$, where $k_1 = k_Z k_C k_{QK} k_Q$. Dividing $\Delta T_1(t)$ by k_1, we reduce it into an input temperature $\Delta T(t) = \Delta T g_1(t)$ and, based on (9), come to the "static" frequency transient

$$\delta f_1(t) = d_1\Delta T_1(t) + d_2\Delta T_1^2(t) + d_3\Delta T_1^3(t), \qquad (18)$$

where

$$\Delta T_1(t) = T_B - T_0 + \Delta T g_1(t), \qquad (19)$$

T_B is a value of $T(t)$ at a start point, d_1, d_2, and d_3 are approximation coefficients.

Function of a frequency thermal transient

It follows from the model (Fig.2) that the thermally induced frequency transient may be written as a sum of "dynamic" and "static" parts

$$\delta f(t) = \delta f_D(t) + \delta f_1(t), \qquad (20)$$

Let us find out the expression for the transient function (20). We sum (14) and (18) and get finally a thermally induced transient

$$\delta f(t) = d_1\Delta T_1(t) - S_D\Delta T\left(v_1 e^{-\frac{t-\tau_Z}{\tau_C}} + v_2 e^{-\frac{t-\tau_Z}{\tau_{QK}}} + v_3 e^{-\frac{t-\tau_Z}{\tau_{Q0}}}\right), + d_2\Delta T_1^2(t) + d_3\Delta T_1^3(t) \qquad (21)$$

where $\Delta T_1(t)$ is obtained by (19), $S_D = S_R k_Z k_C k_{QK}$ is a thermal dynamic coefficient coupled with the Ballato's coefficients $\tilde{a}$ by the relationship [19]

$$\tilde{a} = -S_D\frac{\tau_{Q0}(\tau_{QK}-\tau_C)(\tau_{Q0}-\tau_C)(\tau_{Q0}-\tau_{QK})}{\tau_C^2(\tau_{Q0}-\tau_{QK}) + \tau_{Q0}^2(\tau_{QK}-\tau_C) - \tau_{QK}^2(\tau_{Q0}-\tau_C)}. \qquad (22)$$

Let us conclude that Ballato's coefficient $\tilde{a}$ corresponds to an average temperature of resonator.

Thus, we have worked out the model (21) of thermally induced frequency transient for vacuum-enclosed resonators as reaction to a temperature step. The model, being coupled with Ballato's form, has a universal character and may be used for the prediction of thermal transient for principal and anharmonic modes. We use the model (21) in this paper to get analysis of the anharmonic aging sensor only.

Experimental Verification of the Model

In this section we compare calculated curves defined by (21) with experimental data for the crystal standard based on the vacuum-enclosed AT-cut resonator of PK-187 type. The oven temperature of the standard was sustained at the point $T_{ov} = 65°C$, corresponding to the upper turnover temperature of the mode h_{511} with the principal frequency f_p = 5 MHz. At this point, the anharmonic mode h_{513} ($f_a \cong 5.16$ MHz), excited by modulation [1], has slope ~1 Hz/K of its frequency-temperature characteristic.

To generate thermal transients of the aging sensor frequency $F = f_a - f_p$, the standard was placed into a temperature oven. The approximation coefficients of the aging sensor static frequency-temperature characteristic (19) within the operation temperature range from 0°C to 50°C and with $T_0 = 20°C$ had been found in accordance with the methodology [19] and had the values of

$d_1 = 7.226\times10^{-12}/\mathrm{K}$, $d_2 = -1.886\times10^{-11}/\mathrm{K}^2$, and

$$d_3 = 7.74 \times 10^{-14} / \mathrm{K}^3. \quad (23)$$

Step-by-step changes of ambient temperature caused the standard to respond to and brought the aging sensor frequency from one point of the frequency-temperature characteristic to another by the transient law. Let us give the final results for the average response times and thermal dynamic coefficient for the frequency F [19].

$$\tau_Z = 4.6742\,\mathrm{min}, \quad (24)$$

$$\tau_C = 4.2216\,\mathrm{min}, \quad (25)$$

$$\tau_{QK} = 3.7453\,\mathrm{min}, \quad (26)$$

$$\tau_{Q0} = 16.321\,\mathrm{min}, \quad (27)$$

$$S_D = (-0.28 + 0.21T) \times 10^{-10} / \mathrm{K}. \quad (28)$$

Figure 3 shows, for example, the measurement data as well as approximation and prediction curves for thermal transients in the high temperature range. The other results may be found in [19] respected to the low and middle temperature ranges. Also shown are the anticipated errors of digital filtering of temperature influence determined as calculation minus data. One may see from these figures, and this is expected, that the individually found approximation function best fit the data.

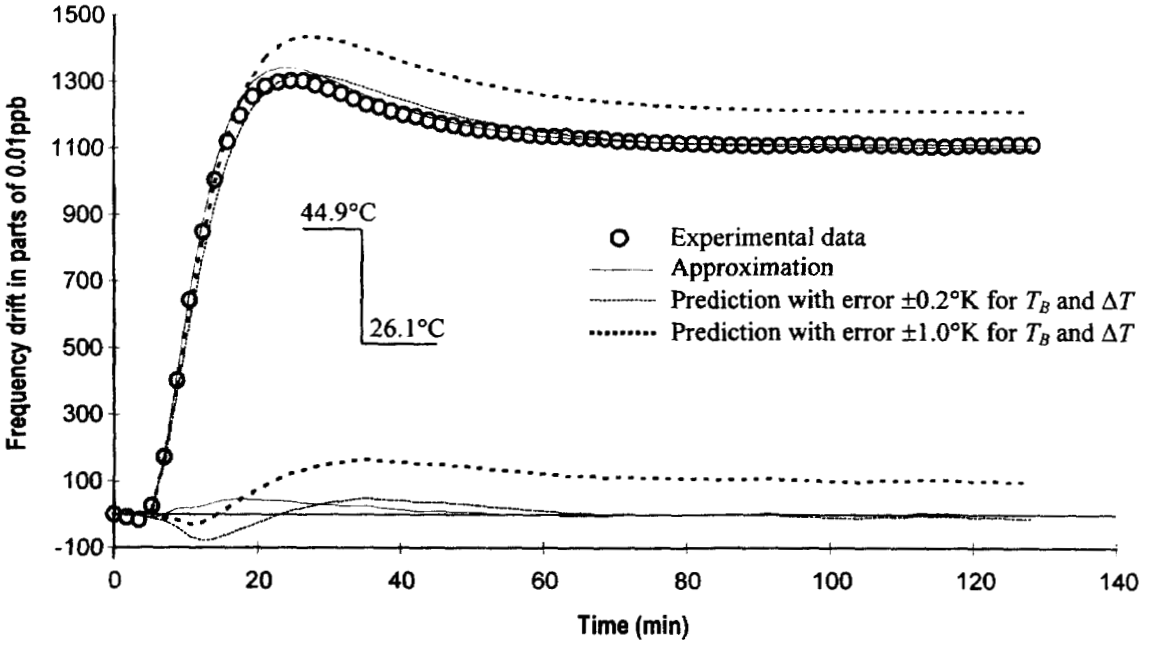

Figure 3. Frequency thermal transients and errors of approximation and prediction in the high temperature range

The prediction curve (Fig. 3) was obtained by (21), assuming either accurate (±0.2°K) or coarse (±1°K) errors of T_B and ΔT measurement. Let us add, the assumption of coarse temperature errors coarse significant errors in the predictions for the high (Fig. 3) and low [19] temperature ranges. In the middle range [19], this error is less visible.

Digital Filtering of an Aging Sensor Thermal Error

In the following studies, we use function (21) with known parameters (23)—(28) of the transient (Fig. 3) to compensate thermal dependence of a frequency $F(T,t)$ of an aging sensor of the crystal standard based on the modulational method. We assume to use the results to develop correspondent software of the standard.

In such type of standards [15], both the principal and aging sensor frequencies f_p =5 MHz and $F = f_a - f_p \approx 0.16$ MHz are formed. An ambient temperature $T(t)$ influences the standard, and of small inertia a crystal sensor, LC-cut, measures this influence (Fig. 4) providing the temperature code $N_T(t)$.

To estimate efficiency of the digital filtering of temperature influence, we introduce a computer-based simulation block and calculate anticipated behavior of the temperature-free frequency of the aging sensor.

The simulation block operates by the following way.

We take samplings of the temperature code $N_T(t)$ and form the temperature-dependent digital sequence x_n. Using a frequency meter with a reference rubidium standard, we form also samplings $F_n(T,t)$ of the sensor frequency $F(T,t)$.

Based on (21) and (22)—(28), we form the temperature transient response of the sensor frequency

$$g_n = \frac{F_n - F_0}{F_N - F_0}, \quad (29)$$

where F_N is (21) for the steady state mode.

We then come to the impulse response

$$h_n = \frac{g_n - g_{n-1}}{T_{sn}}, \quad (30)$$

where T_{sn} = (100...1000)sec is n-th time sampling interval formed by a sensor frequency F.

As we know x_n and h_n, then we calculate convolution

$$y_n = \sum_{k=0}^{n} x_k h_{n-k} \quad (31)$$

and reduce it to the sensor frequency aging as follows. We calculate the scale coefficient

$$k_{sc} = \frac{F_N - F_0}{\Delta T} \quad (32)$$

where ΔT is step of an ambient temperature, and get

$$F'_n(T) = k_{sc} y_n + k_{cal}, \quad (33)$$

where k_{cal} is the calibration coefficient (integration constant). Finally, we calculate the temperature-free samplings $F'_n(t)$ of the sensor frequency $F(T,t)$ and come to the compensated frequency $F(t)$ of the aging sensor

$$F_n(t) = F_n(T,t) - F'_n(T). \quad (34)$$

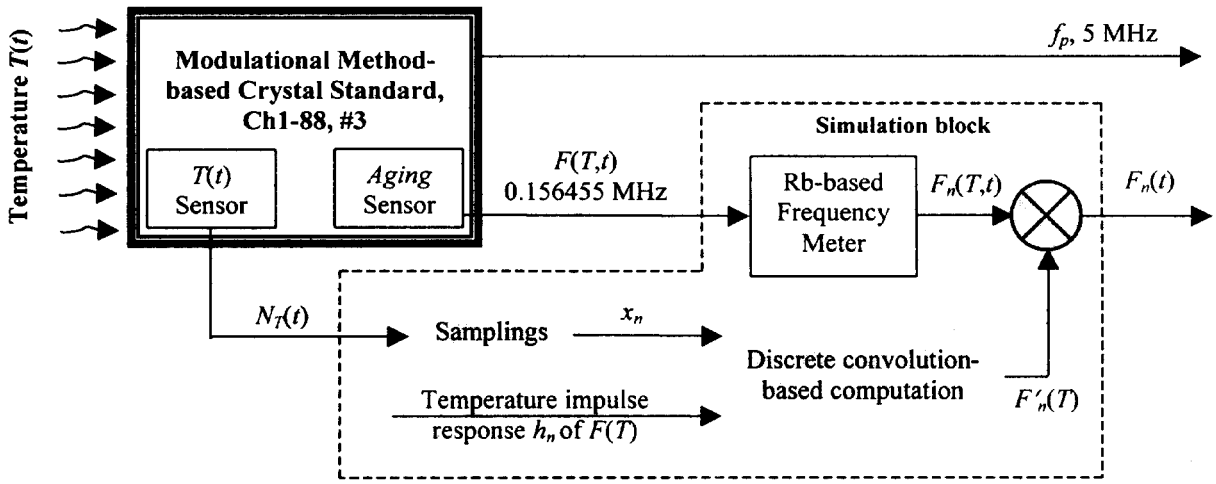

Figure 4. Compensation of a temperature dependence of an aging sensor frequency for a modulational method-based crystal standard

Temperature dependence compensation of the aging sensor frequency

Let us consider results of the temperature dependence compensation of the aging sensor frequency based on discrete convolution.

At the early stage, just before the measurements, we made control of the standard frequency for the reference rubidium source with the temperature 20°C inside the temperature oven and set the frequency with the error of some parts of 10^{-12}. We started to measure through several hours. During this while the frequency $F(T,t)$ had been shifted up to 82×10^{-12} so that at the start point we had 24.6°C.

Fig. 5 shows the plot of the ambient temperature influencing the crystal standard inside the temperature oven. During the first hour of studies, the temperature had been under the oven control only. After that, we changed the temperature to get a dynamic splash and a slowly changed temperature range.

Fig. 6 shows the results of measurement, simulation, and compensation $F_n(T,t)$, $F'_n(T)$, and $F_n(t)$, respectively, presented as continuous functions $F(T,t)$, $F'(T)$, and $F(t)$, respectively.

Considering Fig. 3, we assume that the transient is finished by 1 hour and take this duration as the length of the impulse response (28). Correspondingly, we dropped the processed data obtained during the first hour because of transient. We also fitted the calibration coefficient k_{cal} = 76×10^{-12} to obtain equality of the measured and simulated curves at the point of t = 1hour.

Let us carry out an analysis of all the obtained functions (Fig. 6).

- Both "Static" and "Dynamic" temperature dependences of the frequency of an aging sensor can be predicted based on discrete convolution.
- There are too small data during the first hour of the process of a convolution-based computation that causes a significant prediction error. Thus, the initial transient range should be dropped to avoid compensation errors. As a result, a time delay is appeared.
- A simulated curve $F'(T)$ obtained by convolution exhibits inertia with respect to that of the measured data. The impulse response length of the crystal standard causes inertia that cannot be reduced in practice, as a rule.
- The temperature sensor inertia and inaccuracy of the impulse response measurement led to inaccuracy of

the frequency prediction. Thus, of small inertia a temperature oven and a temperature sensor inside the crystal standard should be used.

- Fast frequency changes cannot be predicted based on convolution because of a big length of the temperature impulse response of the crystal oscillator.

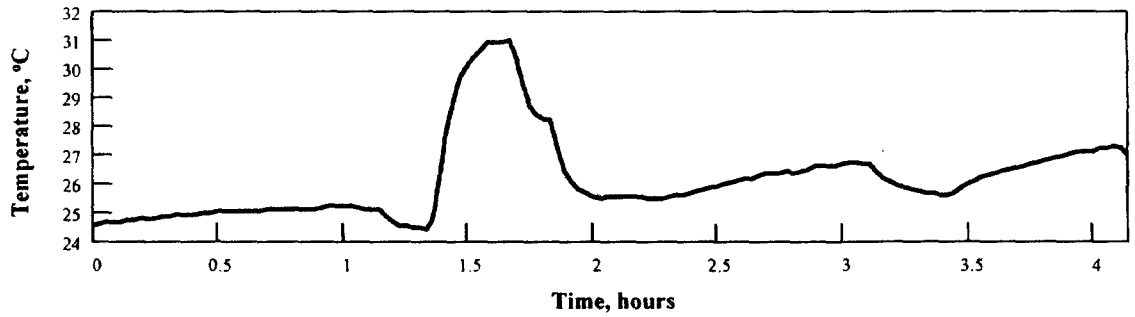

Figure 5. Function of the ambient temperature $T(t)$ influencing the crystal standard

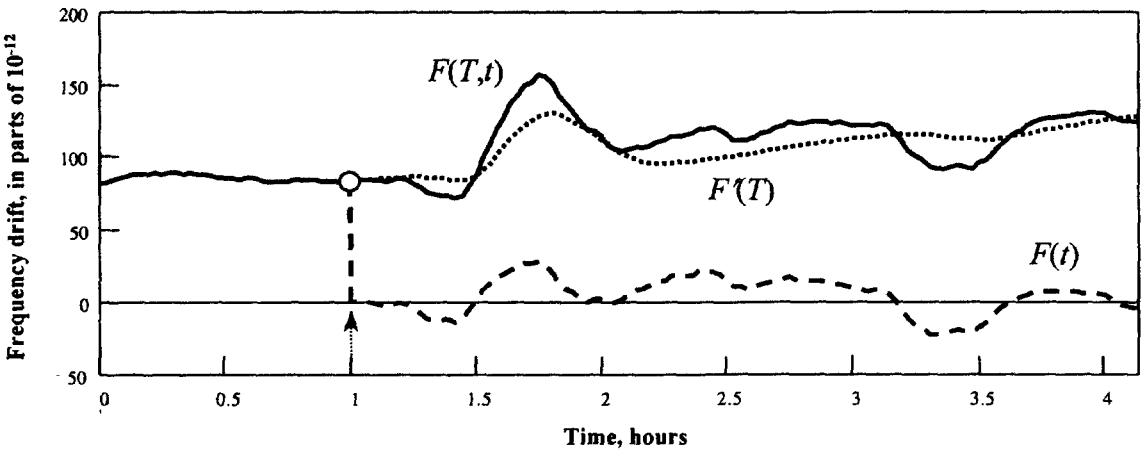

Figure 6. Effects of the ambient temperature (Fig. 5) compensation: $F(T,t)$ is the measured temperature-dependent frequency of the anharmonic aging sensor, $F'(T)$ is the simulated temperature-dependent frequency, and $F(t)$ is the compensated temperature-free frequency

The results implementation into the standard

In reality, in the crystal standard based on the modulational method [15], one deal with the temperature-dependent code of aging obtained by the principal frequency and that of the aging sensor. Naturally, all above given justification should be applied to the aging code because in this case one deal with software only. Let us show how to do it.

An aging code is formed as follows. Based on a sensor frequency, we form the time interval T_{sn} and fill it by the pulses of a principal frequency. Thus, we get

$$N_n(t,T) = \frac{kf_{pn}(t,T)}{F_n(t,T)}, \qquad (35)$$

where k is coefficient to obtain T_{sn} = (100...1000)sec.

We present (35) by the following way

$$N_n = \frac{k(f_{pn} + \Delta f_{pn})}{F_n + \Delta F_n}, \qquad (36)$$

where Δf_{pn}, $\Delta F_n = \Delta f_{an} - \Delta f_{pn}$, and Δf_{an} are temperature-dependent parts of principal, sensor, and anharmonic frequencies, respectively. We assume $\Delta f_p << f_p$, $\Delta f_a << f_a$, and $\Delta f_p << \Delta f_a$, because f_p is ovenized, and get

$$N_n(t,T) \cong \frac{kf_{pn}(t)}{F_n(t)}\left(1 - \frac{\Delta F_n(T)}{F_n(t)}\right) = N_{1n}(t) + N_{2n}(T), \qquad (37)$$

where $N_{1n}(t)$ is sampling of an aging-dependent code $N_1(t) = kf_p(t)/F(t)$, $N_{2n}(T)$ is sampling of a temperature-dependent add to the code

$$N_2(T) \cong -\frac{kf_p}{\bar{F}^2}\Delta F(T), \qquad (38)$$

where f_{pn} and $\bar{F}$ are averaged principal and sensor frequencies.

It follows from (38) consideration that compensation algorithm (29)—(34) may be applied to the aging code of the standard that equals the thermal frequency shift multiplied by the constant (35). Hence, to implement the compensation algorithm into the standard software one should measure the thermal transient of the aging code, form correspondent impulse response, calculate convolution of the code and the ambient temperature, and derive the result from the current code with delay to the transient.

Conclusion

These studies have allowed us to formulate the following conclusions. A model (21) is effective for the prediction of thermally induced frequency transients in an OCXO and crystal standards based on vacuum-enclosed crystal resonators. Major parameters of a model are response times $\tau_Z, \tau_C, \tau_{QK}$, and τ_{Q0}, a thermal dynamic coefficient S_D, and coefficients of a static temperature-to-frequency characteristic d_1, d_2, and d_3. All the parameters are constant and defined by experimentally.

The effectiveness of the digital filtering of the temperature may be estimated based on the Fig. 6. It strongly depends on measurement inaccuracy of the ambient temperature and the temperature impulse response of the standard. Length of the impulse response strongly affects the error as well and causes the time delay.

Despite of inaccuracy of the approach, in whole, we get progress on a way of self-contained aging compensation in the crystal standard.

References

1. Shmaliy, Yuriy S. (1991), "The Modulation Method of the Precision Quartz Crystal Oscillators and Standards Frequency Stabilization", *Proc. of IEEE Int. Freq. Contr. Symp.*, pp.579-589.
2. Shmaliy, Yuriy S., Kurochka O. Ph., Sokolinskiy E. G., and Marienko A. V. (1998), "Quartz Crystal Oscillator with an Effective Aging Rate Compensation," *Proc. 12th European Freq. Time Forum,* Warsaw, Poland, pp.234-239.
3. Ivlev, Leonid I. (1965), "On a Thermal Dynamic Coefficient of a Resonator Frequency", *Voprosy radioelektroniki, Seria 3, Detali i komponenty apparatury*, vol.2, 1965, pp.32-39.
4. Ballato, Arthur, (1979), "Static and Dynamic Behaviour of Quartz Resonators", *in IEEE Trans. Sonics and Ultrason.*, vol.26, June, pp.299-306.
5. Holland, R. (1974), "Non Uniformly Heated Anisotropic Plates: I Mechanical Distortion and Relaxation", *IEEE Trans. Sonics and Ultrason.*, vol.21, May, pp.171-179.
6. ——, (1974), "Non Uniformly Heated Anisotropic Plates: II Frequency Transients in AT and BT Quartz Plates", *Proc. of IEEE Ultrason. Symp.*, pp.582-591.
7. Stevens, D.S., and Tiersten H.F. (1980), "Transient Thermally Induced Frequency Excursions in AT- and SC-Cut Quartz Trapped Energy Resonators," *Proc. 34th IEEE Annu. Freq. Contr. Symp.*, pp.208-217.
8. Janiaud, D., Besson, R., Gagnepain J.J., Valdois, M. (1981), "Quartz Resonator Thermal Transient due to Crystal Support," *Proc. 35th IEEE Annu. Freq. Contr. Symp,* pp.340-344.
9. Valentin, J.P., Theobald, G., Gagnepain J.J. (1984), "Frequency Shifts Arising from in-Plane Temperature Gradient Distribution in Quartz Resonators," *in Proc. 38th IEEE Annu. Freq. Contr. Symp,*, pp.157-163.
10. Valentin, J.P. (1984), "Thermal Gradient Distributions in Trapped Energy Quartz Resonator," *J.Appl. Physic,* p.128.
11. Valentin, J.P., Decailliot, M.D., Besson, R.J. (1984), "New Approach of Fast Warm-Up for Crystal Resonators and Oscillators," *Proc. of 38th IEEE Annu. Freq. Contr. Symp.*, pp.366-373.
12. Yevdokimenko, Yuriy, I., Shmaliy Yu.S. (1991), "Thermal Dynamic Frequency Instability of Crystal Oscillators," *Izvestiia VUZov, Radioelectronika,* No.5, pp.49-55.
13. ——, (1992), "Thermal Dynamic Frequency Instability of Bulk Acoustic Vibrations of Quartz Crystal Piezo Plate", *Akustichesky Jurnal*, vol.38, No.2, pp.283-289.
14. ——, (1993), "A Thermodynamic Resonance in Piezoelectric Crystal Plates of Thickness-Shear Vibrations," *Proc. of 47th IEEE Int. Freq. Contr. Symp.*, pp.193-201.
15. Shmaliy, Yuriy, S. (1998), "The Modulational Method of Quartz Crystal Oscillator Frequency Stabilization," *IEEE Trans. Ultrason., Ferroelect., Freq. Contr.*, vol.45, Nov., pp.1476-1484.
16. Rataiski, J.M. (1968), "Force-Frequency Coefficient of Singly Rotated Vibrating Quartz Crystals," *IBM J.Res.Dev.*, No.1(12), pp.92-99.
17. Stevens, D.S., Tiersten H.F. (1985), "An Analysis of Doubly-Rotated Contoured Quartz Crystal Resonators," *Proc. of 39th IEEE Annu. Freq. Contr. Symp.*, pp.436-447.
18. Shmaliy, Yuriy, S. (1998), "New Thermal Transient Model of Crystal Resonator of Thickness Shear Vibrations," *Proc. 12th European Freq. Time Forum,* Warsaw, Poland, 1998, pp.362-367.
19. Shmaliy, Yuriy, S., Kurochka O.Ph., Sokolinskiy E.G., and Rudnev O.E. (1999), "Thermal Transient Model of a Crystal Resonator Employing Thickness-Shear Vibrations", *IEEE Trans. Ultrason., Ferroelect., Freq. Contr.*, vol.46, Nov., pp.1396-1406.